
Dataset Size Dependence of Rate-Distortion Curve and Threshold of Posterior Collapse in Linear VAE

Yuma Ichikawa

University of Tokyo, Fujitsu Laboratories

Koji Hukushima

University of Tokyo

Abstract

In the Variational Autoencoder (VAE), the variational posterior often aligns closely with the prior, which is known as posterior collapse and hinders the quality of representation learning. To mitigate this problem, an adjustable hyperparameter β has been introduced in the VAE. This paper presents a closed-form expression to assess the relationship between the β in VAE, the dataset size, the posterior collapse, and the rate-distortion curve by analyzing a minimal VAE in a high-dimensional limit. These results clarify that a long plateau in the generalization error emerges with a relatively larger β . As the β increases, the length of the plateau extends and then becomes infinite beyond a certain β threshold. This implies that the choice of β , unlike the usual regularization parameters, can induce posterior collapse regardless of the dataset size. Thus, β is a risky parameter that requires careful tuning. Furthermore, considering the dataset-size dependence on the rate-distortion curve, a relatively large dataset is required to obtain a rate-distortion curve with high rates. Extensive numerical experiments support our analysis.

1 INTRODUCTION

Deep latent variable models are generative models that convert latent variables generated from a prior distribution into samples that closely resemble the data through a neural network. Variational autoencoders (VAE) (Kingma and Welling, 2013; Rezende et al., 2014), one of the deep latent variable models, have been applied in various fields such as image generation (Child, 2020; Vahdat and Kautz, 2020), text generation (Bowman et al., 2015), music generation (Roberts et al., 2018), clustering (Jiang et al., 2016), dimensionality reduction (Akkari et al., 2022), data aug-

mentation (Norouzi et al., 2020), and anomaly detection (An and Cho, 2015; Park et al., 2022). However, direct likelihood maximization is intractable due to the marginalization of latent variables. Consequently, VAE often employs the evidence lower bounds (ELBO), which serve as computable lower bounds on the log-likelihood.

From an information-theoretical point of view, the ELBO has been interpreted in various studies (Alemi et al., 2018; Huang et al., 2020; Nakagawa et al., 2021), which emphasize that the ELBO can be decomposed into two terms representing a trade-off relationship. Drawing an analogy from the rate-distortion theory, these terms can be likened to ‘rate’ and ‘distortion’ (Alemi et al., 2018). Furthermore, these studies suggest that during learning with ELBO, the variational posterior for latent variables tends to align with their prior, hindering effective learning of data representation. This phenomenon is commonly referred to as ‘posterior collapse’.

To address the posterior collapse, an additional parameter, denoted as β_{VAE} , is introduced to control the trade-off between rate and distortion (Higgins et al., 2016); While models with a small β_{VAE} effectively reconstruct data points, i.e., have low distortion, they may generate inauthentic data due to significant mismatches between the variational posteriors and their priors (Alemi et al., 2018). Conversely, models with a large β_{VAE} closely align their variational distributions with the prior, i.e., it has a low rate, but may ignore the encoding critical information. Thus, careful tuning of β_{VAE} in beta-VAEs is important for various applications (Kohl et al., 2018; Castrejon et al., 2019). Moreover, β_{VAE} is intricately linked to disentanglement quality, generalization property, data compression, and posterior collapse. However, theoretical understanding of the relationship between β_{VAE} , the posterior collapse, and the rate-distortion curve has remained limited. Understanding these relationships is essential for practical application and further improvements.

In this study, we clarify the relationship using a minimal model, referred to as Linear VAE (Lucas et al., 2019), which captures the essence of beta-VAEs. Our results show that β_{VAE} significantly affects the generalization performance and the rate-distortion curve. In particular, depend-

ing on β_{VAE} , the generalization performance becomes poor even when provided with abundant data, raising substantial concerns for real-world applications.

Contributions. In our paper, we advance the theory concerning the relationship between the posterior collapse, the rate-distortion curve, and the dataset size. Throughout the manuscript, we consider a high-dimensional limit where the number of training data P and the dimension N are large ($N, P \rightarrow \infty$) while remaining comparable, i.e., $\alpha \triangleq N/P = \Theta(1)$. Our main contributions are:

- A sharp closed-form formula is derived for the generalization properties and the measure of posterior collapse as a function of sample complexity α and β_{VAE} .
- A phenomenon is observed where the generalization error has a peak at a certain sample complexity for a small β_{VAE} . As β_{VAE} increases, the peak continuously decreases, which is remarkably similar to the well-known interpolation peak in supervised regression problems for the regularization parameter (Oppen and Kinzel, 1996; Mignacco et al., 2020; Hastie et al., 2022).
- Our analysis shows that a long plateau in the generalization error exists with respect to sample complexity, α for a large β_{VAE} . As β_{VAE} increases, the length of the plateau increases, and then eventually the length of the plateau is infinite regardless of the value of the sample complexity.
- Using macroscopic variables naturally introduced from replica analysis, we characterize three distinct phases, with the phase diagram pinpointing the boundary of the posterior collapse.
- In the infinite dataset-size limit, the rate-distortion curve of VAE, introduced from the analogy of the rate-distortion theory by Alemi et al. (2018), is confirmed to coincide exactly with that of the Gauss sources (Cover, 1999). In addition, the rate-distortion curve is evaluated as a function of sample complexity α , revealing that a relatively large dataset is required to obtain the optimal rate-distortion curve in the high-rate and low-distortion regions.

Note that all the results are based on the replica method, which is quite standard in statistical physics and is generally believed to be exact, although not rigorous. Thus, the results are presented here as claims.

1.1 Preliminaries

Here we summarize the notations used in this paper. The expression $\|\cdot\|_F$ is Frobenius norm. The notation \oplus denotes the horizontal concatenation of vectors; for vectors

$\mathbf{a} \in \mathbb{R}^N$ and $\mathbf{b} \in \mathbb{R}^M$, $\mathbf{a} \oplus \mathbf{b} = (a_1, \dots, a_N, b_1, \dots, b_M) \in \mathbb{R}^{N+M}$. $I_N \in \mathbb{R}^{N \times N}$ denotes an $N \times N$ identity matrix, and $\mathbf{1}_N$ denotes the vector $(1, \dots, 1)^\top \in \mathbb{R}^N$ and $\mathbf{0}_N$ denotes the vector $(0, \dots, 0)^\top \in \mathbb{R}^N$. $Dx = e^{-x^2/2}/\sqrt{2\pi}dx$ is the standard Gaussian measure. $D_{\text{KL}}[\cdot|\cdot]$ is the Kullback–Leibler (KL) divergence. For a matrix $A = (A_{ij}) \in \mathbb{R}^{N \times M}$ and a vector $\mathbf{a} = (a_i) \in \mathbb{R}^N$, we use the shorthand expression $dA \triangleq \prod_{i=1}^N \prod_{j=1}^M dA_{ij}$ and $d\mathbf{a} \triangleq \prod_{i=1}^N da_i$, respectively.

2 BACKGROUND

2.1 Variational Autoencoders

A VAE (Kingma and Welling, 2013) is a latent generative model. Let $\mathcal{D} = \{x^\mu\}_{\mu=1}^P$ be training data with $x^\mu \in \mathbb{R}^D$ and $p_{\mathcal{D}}(x)$ be the empirical distribution of the training dataset. In practical applications, VAEs are commonly trained using β -VAE objective (Higgins et al., 2016) defined by

$$\mathbb{E}_{p_{\mathcal{D}}} [\mathbb{E}_{q_\phi} [-\log p_\theta(\mathbf{x}|\mathbf{z})] + \beta_{\text{VAE}} D_{\text{KL}}[q_\phi(\mathbf{z}|\mathbf{x})||p(\mathbf{z})]] \triangleq \mathbb{E}_{p_{\mathcal{D}}} [\mathcal{L}(\theta, \phi; \mathbf{x}, \beta_{\text{VAE}})], \quad (1)$$

where $p(\mathbf{z})$ is a prior for the latent variable, and a parameter $\beta_{\text{VAE}} \geq 0$ is introduced to control the trade-off between the first and second terms in Eq. (1). The distributions $p_\theta(\mathbf{x}|\mathbf{z})$ characterized by parameters θ and $q_\phi(\mathbf{z}|\mathbf{x})$ by ϕ are often referred to as *decoder* and *encoder*, respectively. Then, VAEs optimize both the encoder parameters ϕ and decoder parameters θ by minimizing the objective of Eq. (1). Note that when $\beta_{\text{VAE}} = 0$, the objective becomes a deterministic autoencoder, focusing more on minimizing the first term, which is referred to as *reconstruction error*.

2.2 Information-Theoretic Interpretation of VAEs

Alemi et al. (2018); Huang et al. (2020); Park et al. (2022) show that VAEs can be interpreted through the lens of rate-distortion theory (Davisson, 1972; Cover, 1999), which has been successfully applied to data compression. The primary focus has been on the curve where the distortion achieves its minimum value for a given rate, or conversely; see Supplementary Materials B for a detailed explanation. From this perspective, the objective of β -VAEs can be derived from the optimal distortion condition at a given rate.

Drawing an analogy from the rate-distortion theory, Alemi et al. (2018) decompose the β -VAE objective in Eq. (1) into ‘rate’ R and ‘distortion’ D as follows:

$$R(\phi) = \mathbb{E}_{p_{\mathcal{D}}} [D_{\text{KL}}[q_\phi(\mathbf{z}|\mathbf{x})||p(\mathbf{z})]], \quad (2)$$

$$D(\theta, \phi) = \mathbb{E}_{p_{\mathcal{D}}} [\mathbb{E}_{q_\phi} [-\log p_\theta(\mathbf{x}|\mathbf{z})]]. \quad (3)$$

According to Alemi et al. (2018), there exists a trade-off between rate and distortion as in the rate-distortion theory,

especially when encoder and decoder have infinite capacities. This relationship is derived from the identity:

$$H = -\mathbb{E}_{p_{\mathcal{D}}}[D_{\text{KL}}[q_{\phi}(z|\mathbf{x})||p_{\theta}(z|\mathbf{x})]] + R(\phi) + D(\theta, \phi),$$

where H is the data entropy, defined as $H = \mathbb{E}_{p_{\mathcal{D}}}[-\log p_{\mathcal{D}}(\mathbf{x})]$. From the non-negativity of the KL divergence, it follows that $H \leq R(\phi) + D(\theta, \phi)$, where the equality is achieved if and only if the variational posterior and the true posterior coincide, i.e., $\forall \mathbf{x}, q_{\phi}(z|\mathbf{x}) = p_{\theta}(z|\mathbf{x})$.

While this equality holds when the encoder and decoder with infinite capability meet the optimality conditions, the limitation of finite parameters makes this situation unfeasible. Therefore, we aim to find an approximate optimal distortion at a given rate R^* by solving the optimization problem given by

$$\bar{D}(R^*) = \min_{\theta, \phi} D(\theta, \phi) \text{ s.t. } R(\phi) \leq R^*. \quad (4)$$

To optimize without explicitly considering R^* , the Lagrangian function with a Lagrange multiplier $\beta_{\text{VAE}} \geq 0$ can be utilized as

$$\min_{\theta, \phi} D(\theta, \phi) + \beta_{\text{VAE}} R(\phi).$$

This formulation is identical to the β -VAE objective expressed in Eq. (1). Thus, training various VAEs with different β_{VAE} essentially corresponds to distinct points on the rate-distortion curve.

3 SETTING

Generative model for the real data. We consider that real dataset $\mathcal{D} = \{\mathbf{x}^{\mu}\}$ with $\mu = 1, \dots, P$ are drawn according to the generative model given by

$$\mathbf{x}^{\mu} = \sqrt{\frac{\rho}{N}} W^* \mathbf{c}^{\mu} + \sqrt{\eta} \mathbf{n}^{\mu}, \quad (5)$$

where $W^* \in \mathbb{R}^{N \times M^*}$ is a deterministic unknown M^* feature matrix; $\mathbf{c}^{\mu} \in \mathbb{R}^{M^*}$ is a random vector drawn from a standard normal distribution $p(\mathbf{c}) = \mathcal{N}(0_M, I_M)$; \mathbf{n}^{μ} is a background noise vector whose components are i.i.d from the standard normal distribution $\mathcal{N}(0_N, I_N)$; and $\eta \in \mathbb{R}$ and $\rho \in \mathbb{R}$ are scalar parameters to control the strength of the noise and signal, respectively. This generative model, known as the spiked covariance model (Johnstone and Lu, 2009), is used in the theoretical studies of Principal Component Analysis (PCA). Even if W^* is not orthogonal, $W^* \mathbf{c}^{\mu}$ can be rewritten as $(W^* R)(R^{-1} \mathbf{c})$, where R is a matrix that orthogonalizes and normalizes the columns of W^* . This can be viewed as an equivalent system where the new feature vector is $R^{-1} \mathbf{c}$. Therefore, we assume, without loss of generality, that $(W^*)^{\top} W^* = I_M$.

Linear VAE model. In this work, we analyze the following VAE model:

$$p_W(\mathbf{x}|\mathbf{z}) = \mathcal{N}\left(\mathbf{x}; \frac{1}{\sqrt{N}} W \mathbf{z}, I_N\right), \quad (6)$$

$$q_{V,D}(\mathbf{z}|\mathbf{x}) = \mathcal{N}\left(\mathbf{z}; \frac{1}{\sqrt{N}} V^{\top} \mathbf{x}, D\right), \quad (7)$$

$$p(\mathbf{z}) = \mathcal{N}(\mathbf{z}; 0_N, I_N), \quad (8)$$

where the diagonal covariance matrix $D \in \mathbb{R}^{M \times M}$ is learning parameters, and $W \in \mathbb{R}^{N \times M}$ and $V \in \mathbb{R}^{N \times M}$ are also the learning parameters. This model is called linear VAE (Dai et al., 2018; Lucas et al., 2019; Sicks et al., 2021). We assume a fixed identity covariance matrix I_N since this covariance matrix is often used in practice.

The training algorithm. The VAE is trained to learn the generative model by following the optimization problem:

$$\begin{aligned} & (\bar{W}(\mathcal{D}), \bar{V}(\mathcal{D}), \bar{D}(\mathcal{D})) \\ & = \underset{W, V, D}{\operatorname{argmin}} \mathcal{R}(W, V, D; \mathcal{D}, \beta_{\text{VAE}}, \lambda), \end{aligned} \quad (9)$$

where

$$\begin{aligned} \mathcal{R}(W, V, D; \mathcal{D}, \beta_{\text{VAE}}, \lambda) \triangleq & \sum_{\mu=1}^P \mathcal{L}(W, V, D; \mathbf{x}^{\mu}, \beta_{\text{VAE}}) \\ & + \frac{\lambda}{2} \|W\|_F^2 + \frac{\lambda}{2} \|V\|_F^2. \end{aligned}$$

Here $\mathcal{L}(W, V, D; \mathbf{x}, \beta_{\text{VAE}})$ is defined in Eq. (1), and the last two terms regulate the magnitude of the parameters W and V with $\lambda > 0$ being a regularization parameter.

The generalization metric. The VAE can generate a sample $\mathbf{x} \sim p_W(\mathbf{x})$ through the following procedure: First generate a latent variable $\mathbf{z} \sim p(\mathbf{z})$ and then generate a sample $\mathbf{x} \sim p_W(\mathbf{x}|\mathbf{z})$. Thus, the generalization error ε_g is defined as

$$\varepsilon_g(W, W^*) = \frac{1}{N} \mathbb{E}_{\mathbf{c}} \left[\|\sqrt{\rho} W^* \mathbf{c} - W \mathbf{c}\|^2 \right], \quad (10)$$

where $\mathbb{E}_{\mathbf{c}}[\cdot]$ denotes an average over $p(\mathbf{c}) = \mathcal{N}(0_M, I_M)$. The generalization error, ε_g , can measure the extent of signal recovery from the training data.

4 REPLICIA FORMULA

4.1 Replica Formulation

Suppose we define the Boltzmann distribution as

$$p(W, V, D; \mathcal{D}, \beta) \triangleq \frac{1}{Z(\mathcal{D}, \beta)} e^{-\beta \mathcal{R}(W, V, D; \mathcal{D}, \beta_{\text{VAE}}, \lambda, \bar{\lambda})} \quad (11)$$

where $Z(\mathcal{D}, \beta)$ is the normalization constant, known as the partition function in statistical mechanics. Note that in the limit $\beta \rightarrow \infty$, Eq. (11) converges to a distribution concentrated on the $(\bar{W}(\mathcal{D}), \bar{V}(\mathcal{D}), \bar{D}(\mathcal{D}))$. Thus, the expectation of any function $\psi(\bar{W}(\mathcal{D}), \bar{V}(\mathcal{D}), \bar{D}(\mathcal{D}))$ over the dataset can be written by an average over a limiting distribution as

$$\mathbb{E}_{\mathcal{D}} \psi(\bar{W}(\mathcal{D}), \bar{V}(\mathcal{D}), \bar{D}(\mathcal{D})) = \lim_{\beta \rightarrow \infty} \mathbb{E}_{\mathcal{D}} \int dW dV dD \psi(W, V, D) p(W, V, D; \mathcal{D}, \beta).$$

To evaluate this expression, the idea of the replica method (Mézard et al., 1987; Mezard and Montanari, 2009; Blundell, 2022; Zdeborová and Krzakala, 2016) is to compute the cumulant generating function (also known as the free energy density) as

$$f = - \lim_{\beta \rightarrow \infty} \frac{1}{\beta N} \mathbb{E}_{\mathcal{D}} \log Z(\mathcal{D}, \beta). \quad (12)$$

Although Eq. (12) is difficult to calculate straightforwardly, this can be resolved by using the replica method (Mézard et al., 1987; Mezard and Montanari, 2009; Blundell, 2022), which is based on the following equality

$$\mathbb{E}_{\mathcal{D}} \log Z(\mathcal{D}, \beta) = \lim_{n \rightarrow +0} \frac{\log \mathbb{E}_{\mathcal{D}} Z^n(\mathcal{D}, \beta)}{n}. \quad (13)$$

Instead of handling the cumbersome log expression in Eq. (12) directly, one can calculate the average of the n -th power of $Z(\mathcal{D}, \beta)$ for $n \in \mathbb{N}$, analytically continues this expression to $n \in \mathbb{R}$, and finally takes the limit $n \rightarrow +0$. Based on this replica trick, it is sufficient to calculate

$$\begin{aligned} & \mathbb{E}_{\mathcal{D}} Z^n(\mathcal{D}, \beta) \\ &= \mathbb{E}_{\mathcal{D}} \int \prod_{a=1}^n dW^a dV^a dD^a \prod_{a=1}^n e^{-\beta \mathcal{R}(W^a, V^a, D^a; \mathcal{D}, \beta_{\text{VAE}}, \lambda)} \end{aligned}$$

up to the first order of n to take the $n \rightarrow +0$ limit in the right-hand side of Eq. (13).

4.2 Outline of The Derivation

This section provides a brief derivation; see the Supplementary Materials C for comprehensive details. We notice that for every $\mu = 1, \dots, P$, $\mathbf{h}^\mu \triangleq \mathbf{u}^\mu \oplus \tilde{\mathbf{u}}^\mu \in \mathbb{R}^{2Mn}$ with

$$\mathbf{u}^\mu \triangleq \bigoplus_{a=1}^n \frac{1}{\sqrt{N}} (W^a)^\top \mathbf{n}^\mu, \quad \tilde{\mathbf{u}}^\mu \triangleq \bigoplus_{a=1}^n \frac{1}{\sqrt{N}} (V^a)^\top \mathbf{n}^\mu$$

follows a Gaussian multivariate distribution with zero mean $\mathbf{0}_{2Mn}$ and covariance matrix

$$\mathbb{E}_{\mathbf{n}^\mu, \mathbf{n}^\nu} \mathbf{h}^\mu (\mathbf{h}^\nu)^\top = \delta_{\mu\nu} \begin{pmatrix} Q & R \\ R & E \end{pmatrix} \triangleq \delta_{\mu, \nu} \Sigma,$$

$$Q = (Q^{ab}), \quad E = (E^{ab}), \quad R = (R^{ab}),$$

$$Q^{ab} = \frac{1}{N} (W^a)^\top W^b, \quad E^{ab} = \frac{1}{N} (V^a)^\top V^b,$$

$$R^{ab} = \frac{1}{N} (W^a)^\top V^b.$$

Then, one can rewrite

$$\begin{aligned} \mathbb{E}_{\mathcal{D}} Z^n(\mathcal{D}, \beta) &= \int dQ dE dR d\mathbf{m} d\mathbf{d} [\mathcal{S} \times \mathcal{E}], \\ \mathcal{S} &\triangleq \int \prod_{a=1}^n dW^a dV^a \prod_{a,b} \prod_{s,l} \delta \left(Q_{sl}^{ab} - \frac{(\mathbf{w}_s^a)^\top \mathbf{w}_l^b}{N} \right) \\ &\times \delta \left(E_{sl}^{ab} - \frac{(\mathbf{v}_s^a)^\top \mathbf{v}_l^b}{N} \right) \times \delta \left(R_{sl}^{ab} - \frac{(\mathbf{w}_s^a)^\top \mathbf{v}_l^b}{N} \right) \\ &\prod_a \prod_{s,l^*} \delta \left(m_{sl^*}^a - \frac{(\mathbf{w}_s^a)^\top \mathbf{w}_{l^*}^*}{N} \right) \delta \left(d_{sl^*}^a - \frac{(\mathbf{v}_s^a)^\top \mathbf{w}_{l^*}^*}{N} \right) \\ &\times e^{-\frac{\beta}{2} \sum_a (\lambda \|W\|_F^2 + \lambda \|V\|_F^2)}, \\ \mathcal{E} &\triangleq \int \prod_a dD^a \prod_{\mu=1}^P \mathbb{E}_{\mathbf{c}^\mu} \int d\mathbf{h}^\mu \mathcal{N}(\mathbf{h}^\mu, \mathbf{0}_{2Mn}, \Sigma) \\ &\times e^{-\beta \sum_a \mathcal{L}(Q, E, R, m, d; \mathbf{h}^\mu, \mathbf{c}^\mu, \beta_{\text{VAE}}, \lambda, \bar{\lambda})}, \end{aligned}$$

where \mathbf{w}_l^a and \mathbf{v}_l^a are columns vector of W^a and V^a , respectively. We denote $m = (m^a)$ with $m^a = (W^a)^\top W^*/N$ and $d = (d^a)$ with $d^a = (V^a)^\top W^*/N$. Assuming the *replica symmetric* (RS) ansatz, one reads

$$Q_{sl}^{aa} = Q_{sl}, \quad E_{sl}^{aa} = E_{sl}, \quad R_{sl}^{aa} = R_{sl}, \quad (14)$$

$$m_{sl^*}^a = m_{sl^*}, \quad d_{sl^*}^a = d_{sl^*}, \quad (15)$$

$$Q_{sl}^{ab} = Q_{sl} - \chi_{sl}/\beta, \quad (16)$$

$$E_{sl}^{ab} = E_{sl} - \zeta_{sl}/\beta, \quad (17)$$

$$R_{sl}^{ab} = R_{sl} - \omega_{sl}/\beta, \quad (18)$$

where all parameters are denoted as $\Theta \triangleq (Q, E, R, m, d, \chi, \zeta, \omega) \in \mathbb{R}^{M \times (6M+2M^*)}$. The integration of the replicated weight parameters $\{W_a, V_a\}$ over the entire $\mathbb{R}^{(2M \times N) \times n}$ domain is restricted to a subspace that obeys the constraints detailed in Eqs. (21)-(18). Utilizing the Fourier representation of the delta function, the integral \mathcal{S} is further expressed as

$$\begin{aligned} \mathcal{S} &= \int d\hat{Q} d\hat{E} d\hat{R} d\hat{\mathbf{m}} d\hat{\mathbf{d}} e^{\frac{Nn\beta}{2} (\text{tr}(Q\hat{Q} + (n-1)\chi\hat{\chi} - n\beta Q\hat{\chi}))} \\ &\times e^{\frac{Nn\beta}{2} ((\text{tr}(E\hat{E} + (n-1)\chi\hat{\zeta} - n\beta E\hat{\zeta})) + 2(\text{tr}(R\hat{R} + (n-1)\omega\hat{\omega} - n\beta R\hat{\omega}))} \\ &\times e^{N \log \int D\xi_{2M} \left(\int d\tilde{\mathbf{w}} e^{-\beta \left(\frac{1}{2} \tilde{\mathbf{w}}^\top (\hat{Q} + \lambda I_{2M}) \tilde{\mathbf{w}} + (\xi_{2M}^\top \tilde{\chi}^{1/2} + 2_{2M}^\top \tilde{\mathbf{m}}) \tilde{\mathbf{w}} \right)} \right)^n}, \end{aligned}$$

where $\tilde{\mathbf{w}} \triangleq (w_1, \dots, w_M, v_1, \dots, v_M)$ and

$$\tilde{Q} \triangleq \begin{pmatrix} \hat{Q} & \hat{R} \\ \hat{R} & \hat{E} \end{pmatrix}, \quad \tilde{\chi} \triangleq \begin{pmatrix} \hat{\chi} & \hat{\omega} \\ \hat{\omega} & \hat{\zeta} \end{pmatrix}, \quad \tilde{\mathbf{m}} \triangleq \begin{pmatrix} \hat{\mathbf{m}} & \mathbf{0}_{MM^*} \\ \mathbf{0}_{MM^*} & \hat{\mathbf{d}} \end{pmatrix}.$$

Integrating analytically from this expression with respect to $\tilde{\mathbf{w}}$, and under the RS ansatz, the simplified form of \mathcal{E} is obtained as

$$\begin{aligned} \mathcal{E} &= \int D\xi_{2M \times 2M} \\ &\left(\int dV D\mathbf{z}_{2M \times 2M} e^{-\beta \mathcal{L}(\Theta; \mathbf{z}_{2M \times 2M}, \xi_{2M \times 2M}, \beta_{\text{VAE}})} \right)^n. \end{aligned}$$

Furthermore, integrating with respect to Θ by the saddle-point approximation justified for large N limit, and taking the limit $\beta \rightarrow \infty$ after $n \rightarrow +0$ yields eventually the following expression for f .

Claim 4.1. The free energy density f is given by

$$f = \text{extr}_{\Theta} \left\{ -\frac{\text{tr}(Q\hat{Q} - \chi\hat{\chi})}{2} - \frac{\text{tr}(E\hat{E} - \zeta\hat{\zeta})}{2} - \text{tr}(R\hat{R} - \omega\hat{\omega}) + \text{tr}(m\hat{m}) + \text{tr}(d\hat{d}) - \frac{1}{2} \left(\text{tr}[(\hat{\chi}^{\frac{1}{2}})^{\top} (\hat{Q} + \lambda)^{-1} \hat{\chi}^{\frac{1}{2}}] + \mathbf{1}_{2M}^{\top} \hat{m} \hat{Q}^{-1} \hat{m} \mathbf{1}_{2M} \right) + \int D\xi_{2M \times 2M} \min_{D, \mathbf{z}_{2M \times 2M}, \xi_{2M \times 2M}} \mathcal{L}(\Theta, D; \mathbf{z}_{2M \times 2M}, \xi_{2M \times 2M}) \right\},$$

where extr means taking an extremum with respect to Θ .

In particular, when $M = M^* = 1$, the free energy density f can be expressed as follows.

Claim 4.2. When $M = M^* = 1$, the free energy density is given by

$$f = \text{extr}_{\Theta} \left\{ -\frac{1}{2}(\hat{Q}Q - \chi\hat{\chi}) - \frac{1}{2}(\hat{E}E - \zeta\hat{\zeta}) - (\hat{R}R - \omega\hat{\omega}) + \hat{m}m + \hat{d}d + \frac{(\lambda + \hat{E})(\hat{m}^2 + \hat{\chi}) + (\lambda + \hat{Q})(\hat{d}^2 + \hat{\zeta}) - 2\hat{R}(\hat{m}\hat{m} + \hat{\omega})}{2\hat{G}} - \frac{\alpha}{2} \left(\frac{(Q - \eta\chi + \beta_{\text{VAE}})(\rho d^2 + \eta E)}{G} - \frac{\eta\zeta(\rho m^2 + \eta Q)}{G} + \frac{2(\eta\omega - 1)(\rho md + \eta r)}{G} + \beta_{\text{VAE}} \log \frac{Q + \beta_{\text{VAE}}}{\beta_{\text{VAE}}} \right) \right\},$$

where

$$\hat{G} = (\lambda + \hat{Q})(\lambda + \hat{E}) - \hat{R}^2, \\ G = \eta\zeta(Q - \eta\chi + \beta_{\text{VAE}}) + (\eta\omega - 1)^2.$$

From the gradient of the free energy, the extremum conditions are explicitly given by

$$Q = \frac{(\hat{E} + \lambda)\hat{H}}{\hat{G}^2} - \frac{\hat{d}^2 + \hat{\zeta}}{\hat{G}}, \quad E = \frac{(\hat{Q} + \lambda)\hat{H}}{\hat{G}^2} - \frac{\hat{m}^2 + \hat{\chi}}{\hat{G}}, \\ R = -\frac{\hat{R}\hat{H}}{\hat{G}^2} + \frac{\hat{m}\hat{d} + \hat{\omega}}{\hat{G}}, \\ m = \frac{\hat{m}(\hat{E} + \lambda) - \hat{d}\hat{R}}{\hat{G}}, \quad \tilde{m} = \frac{\hat{m}(\hat{E} + \lambda) - \hat{m}\hat{R}}{\hat{G}}, \\ \chi = \frac{\hat{E} + \lambda}{\hat{G}}, \quad \tilde{\chi} = \frac{\hat{Q} + \lambda}{\hat{G}}, \quad \omega = -\frac{\hat{R}}{\hat{G}}, \\ \hat{Q} = \alpha \left(\frac{\beta_{\text{VAE}}}{Q + \beta_{\text{VAE}}} + \frac{\eta Q + d^2\rho - \eta^2\chi}{G} - \frac{\eta\zeta H}{G^2} \right),$$

$$\hat{E} = \alpha\eta \left(\frac{Q - \eta\chi + \beta_{\text{VAE}}}{G} \right), \quad \hat{R} = \alpha\eta \left(\frac{\eta\omega - 1}{G} \right), \\ \hat{\chi} = \alpha\eta \left(\frac{G(\eta E + d^2\rho) - \eta\zeta H}{G^2} \right), \\ \hat{\zeta} = \alpha\eta \left(\frac{G(\eta Q + m^2\rho) - \eta\chi H}{G^2} \right), \\ \hat{\omega} = \alpha\eta \left(\frac{-G(\eta R + md\rho) + (\eta\omega - 1)H}{G^2} \right), \\ \hat{m} = \alpha\rho \left(\frac{\eta m\chi - d(\eta\omega - 1)}{G} \right), \\ \hat{d} = -\alpha\rho \left(\frac{d(Q - \eta\chi + \beta_{\text{VAE}}) + m(\eta\omega - 1)}{G} \right),$$

where

$$\hat{H} = (\lambda + \hat{E})(\hat{m}^2 + \lambda) + (\lambda + \hat{Q})(\hat{d}^2 + \hat{\zeta}) - 2\hat{R}(\hat{m}\hat{d} + \hat{\omega}), \\ H = (d^2\rho + \eta E)(Q - \eta\chi + \beta_{\text{VAE}}) - \eta\zeta(m^2\rho + \eta Q) + 2(\eta R + md\rho)(\rho\omega - 1).$$

Thus, the generalization error and other summary statistics can be evaluated by numerically solving the self-consistent equations.

5 RESULTS

In this section, the generalization properties and the rate-distortion curve are derived from the free energy density obtained in the previous section. In particular, the focus is on the representative case of the simplest VAE, i.e., $M = M^* = 1$. In addition, numerical experiments are conducted to verify the consistency of our theory and to compare the results obtained by training the VAE using a basic gradient descent algorithm.

5.1 Generalization Error and β_{VAE}

We first clarify the relationship between the generalization error and β_{VAE} . Our results can be summarized in three points as follows.

Interpolation peak as in supervised learning. We show that the well-known interpolation peak in supervised regression (Mignacco et al., 2020; Hastie et al., 2022; Opper and Kinzel, 1996) also occurs in VAEs, the unsupervised scenario. The interpolation peak in supervised regression has a characteristic peak in the generalization error at $\alpha = 1$ with a small ridge regularization parameter, and the peak gradually decreases as the regularization parameter increases. Fig. 1 shows the dependence of the generalization error ε_g obtained by the replica method on β_{VAE} and λ , respectively, together with numerical experimental results with finite dataset size. The curves for small β_{VAE}

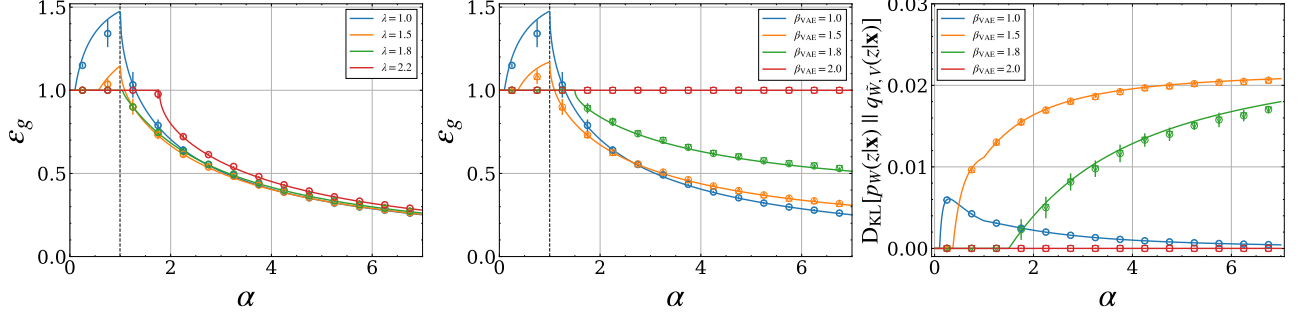


Figure 1: (Left) Generalization error as a function of sample complexity α for fixed parameters $\beta_{\text{VAE}} = 1$ and varying λ (Middle) Generalization error for different β_{VAE} with fixed parameters $\lambda = 1$. (Right) KL divergence between the true posterior and the variational posterior with fixed parameters $\lambda = 1$ for different β_{VAE} . Each data point in all plots represents the average result of five different numerical simulations at $N = 5000$ using gradient descent, and error bars represent standard deviations of the results.

and λ show an peak at $\alpha = 1$. This peak tends to disappear smoothly with increasing β_{VAE} and λ . This result implies that the peak is a universal phenomenon, commonly observed in supervised and unsupervised settings.

Long plateau in ε_g with a large β_{VAE} . The left panel of Fig. (1) shows α dependence of the generalization error ε_g for various β_{VAE} . For a smaller β_{VAE} , the generalization error ε_g begins to decrease from $\alpha = 1$. Meanwhile, as β_{VAE} increases, a long plateau appears in a range of α before the curve begins to decrease. Notably, the length of this plateau gets longer with the increasing values of the β_{VAE} . Moreover, when the value of β_{VAE} exceeds 2, the decrease in the generalization error ε_g seems to disappear completely. The exact points at which the generalization error begins to decrease and remains 1 will be explained in the following section with a corresponding phase diagram description.

The optimal β_{VAE} depends on α and the state closest to the true posterior is not necessarily better. We clarify that the optimal β_{VAE} that minimizes the generalization error ε_g depends on α . Specifically, in a smaller α regime approximately from $\alpha = 1$ to $\alpha \approx 2.6$, the generalization error ε_g is minimized by $\beta_{\text{VAE}} = 1.5$. On the other hand, in the larger α regime, the optimal value is $\beta_{\text{VAE}} = 1$. In addition, the right panel of Fig. (1) shows the KL divergence between the true posterior and the variational posterior, $D_{\text{KL}}[p_W(z|\mathbf{x}) || q_{V,D}(z|\mathbf{x})]$, as a function of α for different values of β_{VAE} . The figure shows that minimizing the generalization error ε_g does not necessarily bring the true posterior $p_W(z|\mathbf{x})$ closer to the variational posterior $q_{V,D}(z|\mathbf{x})$. In fact, even when the generalization error ε_g is minimized at $\beta_{\text{VAE}} = 1.5$, the KL divergence for the β_{VAE} is not minimal in the range about $\alpha = 1$ and $\alpha \approx 2.6$.

5.2 Phase Diagram

In this section, on the basis of the extreme values m and Q in Claim 4.2, we discuss the behavior of β_{VAE} in terms of the phase diagram. Before getting into the analysis of the phase diagram, let us recall the meaning of the order parameters m and q . The order parameter m can be derived to satisfy the equation $m = \mathbb{E}_{\mathcal{D}}[W^{\top} W^* / N]$, where m corresponds to the overlap with the signal W^* and the decoder parameter W . While $m \neq 0$ indicates that the VAE recovers the signal, when $m = 0$, the VAE does not learn the signal, which implies the occurrence of posterior collapse. On the other hand, the relation $q = \mathbb{E}_{\mathcal{D}}[W^{\top} W / N]$ is also derived, meaning that q is the norm of the decoder weights and is the quantity that observes the freedom of the parameter; a smaller q indicates stronger regularization, yielding a smaller effective feasible region of the parameter, while a larger q indicates weaker regularization, yielding the larger effective feasible region. From these parameters, the following three distinct phases are identified, as shown in Fig 2:

- Learning phase (green region, $m \neq 0, q \neq 0$): This phase represents a state where the VAE recovers the signal and avoids posterior collapse.
- Overlearning phase (red region, $m = 0, q \neq 0$): This phase represents a state where the effects of the rate and ridge regularizations are small, resulting in the overlearning of the background noise in the data.
- Regularized phase (orange region, $m = 0, q = 0$): This phase represents a state where the degrees of freedom of the parameters are completely constrained by the rate and ridge regularizations.

The boundaries between the overlearning phase and the learning phase, as well as the regularized phase and the

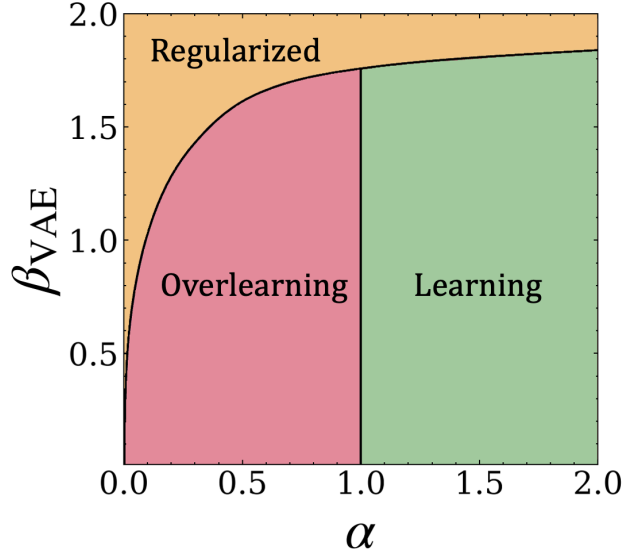


Figure 2: Phase diagram for $\lambda = 1$: Learning phase ($m \neq 0, q \neq 0$), Overlearning phase ($m = 0, q \neq 0$), Regularized phase ($m = 0, q = 0$). The overlearning and regularized phases fail to recover the true signal, which implies the appearance of posterior collapse.

learning phase in the phase diagram, correspond precisely to the point where the generalization error begins to decrease, as noted in the previous section. The phase diagram shows that as β_{VAE} becomes considerably larger, it becomes more difficult to reach the learning phase even with a sufficiently large α , demonstrating the ‘long plateau’ described above.

5.3 Large α limit

The phase diagram in the previous section alone does not allow us to discuss whether it is possible to reach the learning phase by increasing α in any β_{VAE} . In this section, this feasibility is shown from the analysis at a large α limit. Furthermore, the optimal β_{VAE} that minimizes the generalization error in the large α limit is derived in closed form. We first present the following claim:

Claim 5.1. In the large α limit, when $\beta_{\text{VAE}} < \rho + \eta$, the order parameter m and the generalization error ε_g are expressed as

$$m = \sqrt{\rho + \eta - \beta_{\text{VAE}}},$$

$$\varepsilon_g = \rho - \sqrt{\eta + \rho - \beta_{\text{VAE}}}(2\sqrt{\rho} - \sqrt{\eta + \rho - \beta_{\text{VAE}}}),$$

respectively, and when $\beta_{\text{VAE}} \geq \rho + \eta$, $m = 0$ and $\varepsilon_g = 1$.

From Claim 5.1, once β_{VAE} exceeds the threshold $\beta_{\text{VAE}}^* = \rho + \eta$, the learning phase is not reached even if α is increased, which means that the posterior collapse cannot be avoided. Thus, this result suggests that β_{VAE} can be a risky parameter and that learning may fail regardless of

the dataset size. Furthermore, the extremum calculations of the generalization error in Claim 5.1 show that the generalization error reaches a minimum value at $\beta_{\text{VAE}} = \eta$, which means that the best result is achieved when β_{VAE} is equal to the strength of the background noise η .

5.4 Rate-Distortion Curve with Linear VAE

We present results on the rate-distortion curves of VAEs. First, we demonstrate that the following relationship holds in the large α limit.

Claim 5.2. In the large α limit, the rate-distortion curve R_* of the linear VAE equals that of a Gaussian source (Cover, 1999):

$$R_* \triangleq \mathbb{E}_{\mathcal{D}} R(\bar{V}(\mathcal{D}), \bar{D}(\mathcal{D}))$$

$$= \begin{cases} \frac{1}{2} \log \frac{\rho + \eta}{2D_*} & 0 \leq D_* < \frac{\rho + \eta}{2}, \\ 0 & D_* \geq \frac{\rho + \eta}{2}, \end{cases} \quad (19)$$

where D_* is the optimal distortion given by

$$D_* \triangleq \mathbb{E}_{\mathcal{D}} D(\bar{W}(\mathcal{D}), \bar{V}(\mathcal{D}), \bar{D}(\mathcal{D}))$$

$$= \begin{cases} \frac{\beta_{\text{VAE}}}{2} & 0 \leq \beta_{\text{VAE}} < \rho + \eta, \\ \frac{\rho + \eta}{2} & \beta_{\text{VAE}} \geq \rho + \beta_{\text{VAE}}. \end{cases}$$

See the Supplementary Material B for a brief explanation of the rate-distortion function for Gaussian source.

Claim 5.2 suggests that VAE achieves the optimal compression rate in the large α limit. Furthermore, the rate introduced by Alemi et al. (2018) is found to coincide with the rate of discrete quantization of the rate-distortion theorem (Cover, 1999) in the large α limit, indicating that the rate is truly a generalization of the rate of discrete quantization in the rate-distortion theory. The results of the rate-distortion curve in the large α limit and in finite α are shown in Fig. 3. The figure demonstrates that a relatively large dataset is required to obtain the optimal rate-distortion curve in the high-rate and low-distortion regions. Moreover, when $dR(D_*)/dD_* = -1$, VAE achieves the optimal generalization error with $\beta_{\text{VAE}} = \eta$.

6 RELATED WORK

Replica Method. The replica method is a non-rigorous but powerful heuristic of statistical physics (Mézard et al., 1987; Mezard and Montanari, 2009; Blundell, 2022). It has proven to be a valuable method for high-dimensional machine-learning problems. Previous studies have investigated supervised learning: single-layer (Gardner and Derrida, 1988; Opper and Haussler, 1991; Barbier et al., 2019; Aubin et al., 2020) and multi-layer (Aubin et al., 2018) neural networks, as well as kernel methods (Dietrich et al., 1999; Bordelon et al., 2020; Gerace et al., 2020) and unsupervised learning: dimensionality reduction techniques

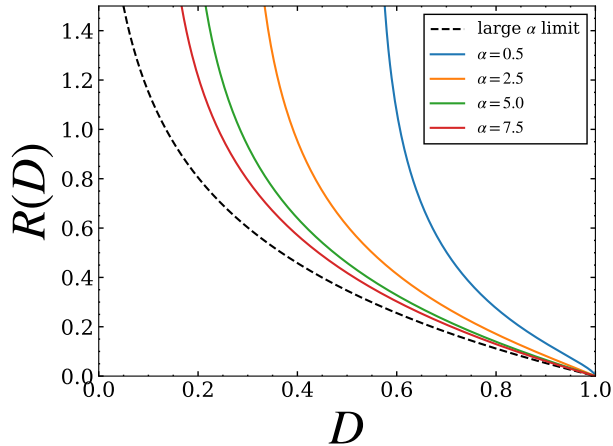


Figure 3: Rate-distortion curve for $\lambda = 1$ with various values of α . The dashed line represents the curve in the limit of infinite α , which coincides with the rate-distortion curve for a Gaussian source (Cover, 1999).

such as principal component analysis (Biehl and Mietzner, 1993; Hoyle and Rattray, 2004, 2007), and generative models such as energy-based models (Decelle et al., 2018; Ichikawa and Hukushima, 2022) and denoising autoencoders (Cui and Zdeborová, 2023). However, there has been no analysis of VAEs, and in this study, we conducted an analysis of VAEs. Efforts have been made to confirm the non-rigorous results of the replica method using other rigorous analysis techniques. For convex optimization problems, the Gaussian min-max theorem (Gordon, 1985) can be used for rigorous analysis, which provides rigorous results consistent with those of the replica method (Thramoulidis et al., 2018).

Linear VAEs. The linear VAE is a simple model where both the encoder and decoder are constrained to be affine transformations (Lucas et al., 2019). While deriving analytical results for deep latent models is often intractable, the linear VAE can provide analytical results, facilitating a deeper understanding of VAEs. Furthermore, despite this simplicity, the theoretical results can well explain the behavior of deeper and intricately structured VAEs (Lucas et al., 2019; Bae et al., 2022). In fact, results proven effective for linear models have been applied to deeper models, leading to the new algorithms (Bae et al., 2022). In addition, various theoretical results have been obtained; Dai et al. (2018) show the connections between linear VAE, probabilistic PCA (Tipping and Bishop, 1999), and robust PCA (Candès et al., 2011; Chandrasekaran et al., 2011). In parallel, studies by Lucas et al. (2019) and Wang and Ziyin (2022) utilize linear VAEs to explore the origins of posterior collapse. However, these analyses do not address the dataset-size dependence of generalization performance, the rate-distortion curve, and the robustness against back-

ground noise examined in our study.

7 CONCLUSION

In this paper, we clarify the relationship between dataset size, β_{VAE} , the posterior collapse, and the rate-distortion curve by using a replica method to evaluate the sharp asymptotic properties of the linear VAE. Building on these results, we observe a peak in the generalization error at a particular sample complexity for small values of β_{VAE} , reminiscent of the well-known interpolation peak in supervised regressions. This suggests that the peak is a universal phenomenon, independent of supervised and unsupervised learning. We also find that a long plateau appears in the generalization error for a large value of β_{VAE} . As β_{VAE} increases, the length of the plateau extends, and when β_{VAE} exceeds a critical value, it goes to infinity even for infinite dataset size. This result suggests that, unlike the ridge regularization parameter, β_{VAE} is potentially risky. Extending the data generative model and the linear VAE to more complex models and analyzing the learning dynamics of the linear VAE are interesting future directions.

References

- Akkari, N., Casenave, F., Hachem, E., and Ryckelynck, D. (2022). A bayesian nonlinear reduced order modeling using variational autoencoders. *Fluids*, 7(10):334.
- Alemi, A., Poole, B., Fischer, I., Dillon, J., Saourous, R. A., and Murphy, K. (2018). Fixing a broken elbow. In *International conference on machine learning*, pages 159–168. PMLR.
- An, J. and Cho, S. (2015). Variational autoencoder based anomaly detection using reconstruction probability. *Special lecture on IE*, 2(1):1–18.
- Aubin, B., Krzakala, F., Lu, Y., and Zdeborová, L. (2020). Generalization error in high-dimensional perceptrons: Approaching bayes error with convex optimization. *Advances in Neural Information Processing Systems*, 33:12199–12210.
- Aubin, B., Maillard, A., Krzakala, F., Macris, N., Zdeborová, L., et al. (2018). The committee machine: Computational to statistical gaps in learning a two-layers neural network. *Advances in Neural Information Processing Systems*, 31.
- Bae, J., Zhang, M. R., Ruan, M., Wang, E., Hasegawa, S., Ba, J., and Grosse, R. (2022). Multi-rate vae: Train once, get the full rate-distortion curve. *arXiv preprint arXiv:2212.03905*.
- Barbier, J., Krzakala, F., Macris, N., Miolane, L., and Zdeborová, L. (2019). Optimal errors and phase transitions in high-dimensional generalized linear models. *Proceedings of the National Academy of Sciences*, 116(12):5451–5460.

- Berger, T., Davisson, L. D., and Berger, T. (1975). Rate distortion theory and data compression. *Advances in Source Coding*, pages 1–39.
- Berger, T. and Gibson, J. D. (1998). Lossy source coding. *IEEE Transactions on Information Theory*, 44(6):2693–2723.
- Biehl, M. and Mietzner, A. (1993). Statistical mechanics of unsupervised learning. *Europhysics Letters*, 24(5):421.
- Blundell, S. J. (2022). Theory of simple glasses: exact solutions in infinite dimensions. *Contemporary Physics*, 62(4).
- Bordelon, B., Canatar, A., and Pehlevan, C. (2020). Spectrum dependent learning curves in kernel regression and wide neural networks. In *International Conference on Machine Learning*, pages 1024–1034. PMLR.
- Bowman, S. R., Vilnis, L., Vinyals, O., Dai, A. M., Jozefowicz, R., and Bengio, S. (2015). Generating sentences from a continuous space. *arXiv preprint arXiv:1511.06349*.
- Brekelmans, R., Moyer, D., Galstyan, A., and Ver Steeg, G. (2019). Exact rate-distortion in autoencoders via echo noise. *Advances in neural information processing systems*, 32.
- Candès, E. J., Li, X., Ma, Y., and Wright, J. (2011). Robust principal component analysis? *Journal of the ACM (JACM)*, 58(3):1–37.
- Castrejon, L., Ballas, N., and Courville, A. (2019). Improved conditional vrns for video prediction. In *Proceedings of the IEEE/CVF international conference on computer vision*, pages 7608–7617.
- Chandrasekaran, V., Sanghavi, S., Parrilo, P. A., and Willsky, A. S. (2011). Rank-sparsity incoherence for matrix decomposition. *SIAM Journal on Optimization*, 21(2):572–596.
- Child, R. (2020). Very deep vaes generalize autoregressive models and can outperform them on images. *arXiv preprint arXiv:2011.10650*.
- Cover, T. M. (1999). *Elements of information theory*. John Wiley & Sons.
- Cui, H. and Zdeborová, L. (2023). High-dimensional asymptotics of denoising autoencoders. *arXiv preprint arXiv:2305.11041*.
- Dai, B., Wang, Y., Aston, J., Hua, G., and Wipf, D. (2018). Connections with robust pca and the role of emergent sparsity in variational autoencoder models. *The Journal of Machine Learning Research*, 19(1):1573–1614.
- Davisson, L. (1972). Rate distortion theory: A mathematical basis for data compression. *IEEE Transactions on Communications*, 20(6):1202–1202.
- Decelle, A., Fissore, G., and Furtlehner, C. (2018). Thermodynamics of restricted boltzmann machines and related learning dynamics. *Journal of Statistical Physics*, 172:1576–1608.
- Dietrich, R., Opper, M., and Sompolinsky, H. (1999). Statistical mechanics of support vector networks. *Physical review letters*, 82(14):2975.
- Gao, W., Liu, Y.-H., Wang, C., and Oh, S. (2019). Rate distortion for model compression: From theory to practice. In *International Conference on Machine Learning*, pages 2102–2111. PMLR.
- Gardner, E. and Derrida, B. (1988). Optimal storage properties of neural network models. *Journal of Physics A: Mathematical and general*, 21(1):271.
- Gerace, F., Loureiro, B., Krzakala, F., Mézard, M., and Zdeborová, L. (2020). Generalisation error in learning with random features and the hidden manifold model. In *International Conference on Machine Learning*, pages 3452–3462. PMLR.
- Gordon, Y. (1985). Some inequalities for gaussian processes and applications. *Israel Journal of Mathematics*, 50:265–289.
- Hastie, T., Montanari, A., Rosset, S., and Tibshirani, R. J. (2022). Surprises in high-dimensional ridgeless least squares interpolation. *Annals of statistics*, 50(2):949.
- Higgins, I., Matthey, L., Pal, A., Burgess, C., Glorot, X., Botvinick, M., Mohamed, S., and Lerchner, A. (2016). beta-vaes: Learning basic visual concepts with a constrained variational framework. In *International conference on learning representations*.
- Hoyle, D. C. and Rattay, M. (2004). Principal-component-analysis eigenvalue spectra from data with symmetry-breaking structure. *Physical Review E*, 69(2):026124.
- Hoyle, D. C. and Rattay, M. (2007). Statistical mechanics of learning multiple orthogonal signals: asymptotic theory and fluctuation effects. *Physical review E*, 75(1):016101.
- Huang, S., Makhzani, A., Cao, Y., and Grosse, R. (2020). Evaluating lossy compression rates of deep generative models. In *International Conference on Machine Learning*, pages 4444–4454. PMLR.
- Ichikawa, Y. and Hukushima, K. (2022). Statistical-mechanical study of deep boltzmann machine given weight parameters after training by singular value decomposition. *Journal of the Physical Society of Japan*, 91(11):114001.
- Isik, B., Weissman, T., and No, A. (2022). An information-theoretic justification for model pruning. In *International Conference on Artificial Intelligence and Statistics*, pages 3821–3846. PMLR.
- Jiang, Z., Zheng, Y., Tan, H., Tang, B., and Zhou, H. (2016). Variational deep embedding: An unsupervised

- and generative approach to clustering. *arXiv preprint arXiv:1611.05148*.
- Johnstone, I. M. and Lu, A. Y. (2009). On consistency and sparsity for principal components analysis in high dimensions. *Journal of the American Statistical Association*, 104(486):682–693.
- Kingma, D. P. and Welling, M. (2013). Auto-encoding variational bayes. *arXiv preprint arXiv:1312.6114*.
- Kohl, S., Romera-Paredes, B., Meyer, C., De Fauw, J., Ledsam, J. R., Maier-Hein, K., Eslami, S., Jimenez Rezende, D., and Ronneberger, O. (2018). A probabilistic u-net for segmentation of ambiguous images. *Advances in neural information processing systems*, 31.
- Lucas, J., Tucker, G., Grosse, R. B., and Norouzi, M. (2019). Don’t blame the elbo! a linear vae perspective on posterior collapse. *Advances in Neural Information Processing Systems*, 32.
- Mezard, M. and Montanari, A. (2009). *Information, physics, and computation*. Oxford University Press.
- Mézard, M., Parisi, G., and Virasoro, M. A. (1987). *Spin glass theory and beyond: An Introduction to the Replica Method and Its Applications*, volume 9. World Scientific Publishing Company.
- Mignacco, F., Krzakala, F., Lu, Y., Urbani, P., and Zdeborova, L. (2020). The role of regularization in classification of high-dimensional noisy gaussian mixture. In *International conference on machine learning*, pages 6874–6883. PMLR.
- Nakagawa, A., Kato, K., and Suzuki, T. (2021). Quantitative understanding of vae as a non-linearly scaled isometric embedding. In *International Conference on Machine Learning*, pages 7916–7926. PMLR.
- Norouzi, S., Fleet, D. J., and Norouzi, M. (2020). Exemplar vae: Linking generative models, nearest neighbor retrieval, and data augmentation. *Advances in Neural Information Processing Systems*, 33:8753–8764.
- Opper, M. and Haussler, D. (1991). Generalization performance of bayes optimal classification algorithm for learning a perceptron. *Physical Review Letters*, 66(20):2677.
- Opper, M. and Kinzel, W. (1996). Statistical mechanics of generalization. In *Models of Neural Networks III: Association, Generalization, and Representation*, pages 151–209. Springer.
- Park, S., Adosoglou, G., and Pardalos, P. M. (2022). Interpreting rate-distortion of variational autoencoder and using model uncertainty for anomaly detection. *Annals of Mathematics and Artificial Intelligence*, pages 1–18.
- Rezende, D. J., Mohamed, S., and Wierstra, D. (2014). Stochastic backpropagation and approximate inference in deep generative models. In *International conference on machine learning*, pages 1278–1286. PMLR.
- Roberts, A., Engel, J., Raffel, C., Hawthorne, C., and Eck, D. (2018). A hierarchical latent vector model for learning long-term structure in music. In *International conference on machine learning*, pages 4364–4373. PMLR.
- Shannon, C. E. et al. (1959). Coding theorems for a discrete source with a fidelity criterion. *IRE Nat. Conv. Rec.*, 4(142-163):1.
- Sicks, R., Korn, R., and Schwaar, S. (2021). A generalised linear model framework for β -variational autoencoders based on exponential dispersion families. *The Journal of Machine Learning Research*, 22(1):10539–10579.
- Theis, L., Salimans, T., Hoffman, M. D., and Mentzer, F. (2022). Lossy compression with gaussian diffusion. *arXiv preprint arXiv:2206.08889*.
- Thrampoulidis, C., Abbasi, E., and Hassibi, B. (2018). Precise error analysis of regularized m -estimators in high dimensions. *IEEE Transactions on Information Theory*, 64(8):5592–5628.
- Tipping, M. E. and Bishop, C. M. (1999). Probabilistic principal component analysis. *Journal of the Royal Statistical Society Series B: Statistical Methodology*, 61(3):611–622.
- Vahdat, A. and Kautz, J. (2020). Nvae: A deep hierarchical variational autoencoder. *Advances in neural information processing systems*, 33:19667–19679.
- Wang, Z. and Ziyin, L. (2022). Posterior collapse of a linear latent variable model. *Advances in Neural Information Processing Systems*, 35:37537–37548.
- Zdeborová, L. and Krzakala, F. (2016). Statistical physics of inference: Thresholds and algorithms. *Advances in Physics*, 65(5):453–552.

Dataset Size Dependence of Rate-Distortion Curve and Threshold of Posterior Collapse in Linear VAE: Supplementary Materials

A OVERVIEW

This supplementary material provides extended explanations, implementation details, and additional results for the paper “Dataset Size Dependence of Rate-Distortion Curve and Threshold of Posterior Collapse in Linear VAE”.

B REVIEW OF RATE DISTORTION THEORY

The rate-distortion theory was introduced by Shannon et al. (1959) and then further developed by Berger et al. (1975); Berger and Gibson (1998). This theoretical framework describes the minimum bit rate (rate) required for encoding a source, subject to a given distortion measure. In recent years, it has been used to understand machine learning (Gao et al., 2019; Alemi et al., 2018; Theis et al., 2022; Brekelmans et al., 2019; Isik et al., 2022).

Let $X^P = \{X_1, \dots, X_P\} \in \mathcal{X}^P$ be i.i.d random variables from the distribution $P(x)$. An encoder $f_P : \mathcal{X}^P \rightarrow \{1, 2, \dots, 2^{P \times R}\}$ maps the input X^P into a quantized vector, and a decoder $g_P : \{1, 2, \dots, 2^{P \times R}\} \rightarrow \mathcal{X}^P$ reconstructs the input by a decoded input \hat{X}^P from the quantized vector. To measure the discrepancy between the original and decoded inputs, a distortion function $d : \mathcal{X} \times \mathcal{X} \rightarrow \mathbb{R}_+$ is introduced. The distortion for the input X^P and decoded input \hat{X}^P is defined as the average distortion between each pair X_i and \hat{X}_i . Commonly used distortion functions are the Hamming distortion function defined as $d(x, \hat{x}) = \mathbb{I}[x \neq \hat{x}]$ for $X = \{0, 1\}$ where \mathbb{I} is the indicator function, and the squared error distortion function defined as $d(x, \hat{x}) = (x - \hat{x})^2$ for $X = \mathbb{R}$. We are ready to define the rate-distortion function.

Definition B.1. A rate-distortion pair (R, D) is achievable if there exists a (probabilistic) encoder-decoder (f_P, g_P) such that the quantized vector has size $2^{P \times R}$ and the expected distortion $\lim_{P \rightarrow \infty} [d(X^P, g_P(f_P(X^P)))] \leq D$.

Definition B.2. The rate-distortion function $R(D)$ is the infimum of rates R such that the rate-distortion pair (R, D) is achievable.

The main theorem of the rate-distortion theory (Cover, 1999) states as follows,

Theorem B.3. Given an upper bound of distortion D , the following equation holds:

$$R(D) = \min_{P(\hat{X}|X): \mathbb{E}[d(X, \hat{X})] \leq D} I(X; \hat{X}) \quad (20)$$

The rate-distortion theorem provides the fundamental limit of data compression, i.e., how many minimum bits are needed to compress the input, given the quality of the reconstructed input.

B.1 Rate-distortion of Gaussian source.

We give an example of the rate-distortion function for Gaussian input.

Proposition B.4. If $X \sim \mathcal{N}(0, \sigma^2)$, the rate-distortion function is given by

$$R(D) = \begin{cases} \frac{1}{2} \log_2 \frac{\sigma^2}{D} & D \leq \sigma^2 \\ 0 & D > \sigma^2 \end{cases}.$$

If the required distortion is larger than the variance of the Gaussian variable σ^2 , we simply transmit $\hat{X} = 0$; otherwise, we transmit \hat{X} such that $\hat{X} \sim \mathcal{N}(0, \sigma^2 - D)$, $X - \hat{X} \sim \mathcal{N}(0, D)$ where \hat{X} and $X - \hat{X}$ are independent.

C DETAILED DERIVATION OF CLAIMS

Here, we present the derivation of Claims 4.1, 4.2, 5.1, and 5.2.

C.1 Derivation of Claim 4.1

To calculate free-energy density, it is sufficient to calculate the replicated partition function, as mentioned in Section 4.1. The replicated partition function is expressed as

$$\begin{aligned}
 \mathbb{E}_{\mathcal{D}} Z^n(\mathcal{D}, \beta) &= \mathbb{E}_{\mathcal{D}} \int \prod_{a=1}^n dW^a dV^a dD^a \prod_{a=1}^n e^{-\beta \mathcal{R}(W^a, V^a, D^a; \mathcal{D}, \beta_{\text{VAE}}, \lambda)} \\
 &= \mathbb{E}_{\mathcal{D}} \int \prod_{a=1}^n dW^a dV^a dD^a \prod_{a=1}^n e^{-\beta \sum_{\mu=1}^P \mathcal{L}(W^a, V^a, D^a; \mathbf{x}^\mu, \beta_{\text{VAE}})} e^{-\beta \left(\frac{\lambda}{2} \|W^a\|_F^2 + \frac{\lambda}{2} \|V^a\|_F^2 \right)} \\
 &= \int \prod_{a=1}^n dW^a dV^a dD^a \prod_{\mu=1}^P \mathbb{E}_{\mathbf{c}^\mu, \mathbf{n}^\mu} \left[\prod_{a=1}^n e^{-\beta \sum_{\mu=1}^P \mathcal{L}(W^a, V^a, D^a; \mathbf{c}^\mu, \mathbf{n}^\mu, \beta_{\text{VAE}})} \right] e^{-\beta \left(\frac{\lambda}{2} \|W^a\|_F^2 + \frac{\lambda}{2} \|V^a\|_F^2 \right)} \\
 &= \int \prod_{a=1}^n dW^a dV^a dD^a \left(\mathbb{E}_{\mathbf{c}, \mathbf{n}} \left[\prod_{a=1}^n e^{-\beta \sum_{\mu=1}^P \mathcal{L}(W^a, V^a, D^a; \mathbf{c}, \mathbf{n}, \beta_{\text{VAE}})} \right] \right)^P e^{-\beta \left(\frac{\lambda}{2} \|W^a\|_F^2 + \frac{\lambda}{2} \|V^a\|_F^2 \right)},
 \end{aligned}$$

where $\mathcal{L}(W^a, V^a, D^a; \mathbf{c}, \mathbf{n}, \beta_{\text{VAE}})$ is given by

$$\begin{aligned}
 \mathcal{L}(W^a, V^a, D^a; \mathbf{c}, \mathbf{n}, \beta_{\text{VAE}}) &= \frac{1}{2} \left(\left\| \sqrt{\frac{\rho}{N}} W^* \mathbf{c} + \sqrt{\eta} \mathbf{n} \right\|^2 \right. \\
 &\quad - \frac{2}{\sqrt{N}} \left(\sqrt{\frac{\rho}{N}} (W^a)^\top W^* \mathbf{c} + \sqrt{\eta} (W^a)^\top \mathbf{n} \right)^\top \left(\frac{\sqrt{\rho}}{N} (V^a)^\top W^* \mathbf{c} + \sqrt{\frac{\eta}{N}} (V^a)^\top \mathbf{n} \right) \\
 &\quad + \left(\frac{\sqrt{\rho}}{N} (V^a)^\top W^* \mathbf{c} + \sqrt{\frac{\eta}{N}} (V^a)^\top \mathbf{n} \right)^\top \frac{(W^a)^\top W^a}{N} \left(\frac{\sqrt{\rho}}{N} (V^a)^\top W^* \mathbf{c} + \sqrt{\frac{\eta}{N}} (V^a)^\top \mathbf{n} \right) + \frac{1}{N} (W^a)^\top W^a D^a \\
 &\quad \left. + \beta_{\text{VAE}} \left(\left\| \frac{\sqrt{\rho}}{N} (V^a)^\top W^* \mathbf{c} + \sqrt{\frac{\eta}{N}} (V^a)^\top \mathbf{n} \right\|^2 + \text{tr}(D^a)^2 - \text{tr}(\log D^a) \right) \right).
 \end{aligned}$$

To perform the average over \mathbf{n} , we notice that, since \mathbf{n} follows a multivariate normal distribution $\mathcal{N}(\mathbf{0}_N, \mathbf{I}_N)$, $\mathbf{h} \triangleq \mathbf{u} \oplus \tilde{\mathbf{u}} \in \mathbb{R}^{2Mn}$ with

$$\mathbf{u}^\mu \triangleq \bigoplus_{a=1}^n \frac{1}{\sqrt{N}} (W^a)^\top \mathbf{n}^\mu, \quad \tilde{\mathbf{u}}^\mu \triangleq \bigoplus_{a=1}^n \frac{1}{\sqrt{N}} (V^a)^\top \mathbf{n}^\mu$$

follows a following Gaussian multivariate distribution:

$$p(\mathbf{h}) = \mathcal{N}(\mathbf{h}; \mathbf{0}_{2Mn}, \Sigma),$$

where

$$\begin{aligned}
 \Sigma &= \delta_{\mu\nu} \begin{pmatrix} Q & R \\ R & E \end{pmatrix}, \quad Q = (Q^{ab}) \in \mathbb{R}^{Mn \times Mn}, \quad E = (E^{ab}) \in \mathbb{R}^{Mn \times Mn}, \quad R = (R^{ab}) \in \mathbb{R}^{Mn \times Mn}, \\
 Q^{ab} &= \frac{1}{N} (W^a)^\top W^b, \quad E^{ab} = \frac{1}{N} (V^a)^\top V^b, \quad R^{ab} = \frac{1}{N} (W^a)^\top V^b.
 \end{aligned}$$

By introducing the auxiliary variables through the trivial identities

$$\begin{aligned}
 1 &= \prod_{(a,l);(b,s)} N \int \delta(NQ_{ls}^{ab} - (\mathbf{w}_l^a)^\top \mathbf{w}_s^b) dQ, \\
 1 &= \prod_{(a,l);(b,s)} N \int \delta(NE_{ls}^{ab} - (\mathbf{v}_l^a)^\top \mathbf{v}_s^b) dE, \\
 1 &= \prod_{(a,l);(b,s)} N \int \delta(NR_{ls}^{ab} - (\mathbf{w}_l^a)^\top \mathbf{v}_s^b) dR, \\
 1 &= \prod_{(a,s);(a,l^*)} N \int \delta(Nm_{sl^*}^a - (\mathbf{w}_s^a)^\top \mathbf{w}_{l^*}^*) dm, \\
 1 &= \prod_{(a,s);(a,l^*)} N \int \delta(Nd_{sl^*}^a - (\mathbf{v}_s^a)^\top \mathbf{w}_{l^*}^*) dd,
 \end{aligned}$$

the replicated partition function is further expressed as

$$\begin{aligned}
 \mathbb{E}_{\mathcal{D}} Z^n(\mathcal{D}, \beta) &= \int dQ dE dR d m d d [\mathcal{S} \times \mathcal{E}], \\
 \mathcal{S} &\triangleq \int \prod_{a=1}^n dW^a dV^a \prod_{a,b} \prod_{s,l} N \delta(NQ_{sl}^{ab} - (\mathbf{w}_s^a)^\top \mathbf{w}_l^b) N \delta(NE_{sl}^{ab} - (\mathbf{v}_s^a)^\top \mathbf{v}_l^b) N \delta(NR_{sl}^{ab} - (\mathbf{w}_s^a)^\top \mathbf{v}_l^b) \\
 &\quad \prod_a \prod_{s,l} N \delta(Nm_{sl^*}^a - (\mathbf{w}_s^a)^\top \mathbf{w}_{l^*}^*) N \delta(d_{sl^*}^a - (\mathbf{v}_s^a)^\top \mathbf{w}_{l^*}^*) \times e^{-\frac{\beta}{2} \sum_a (\lambda \|W\|_F^2 + \lambda \|V\|_F^2)}, \\
 \mathcal{E} &\triangleq \int \prod_a dD^a \left(\int Dc \int d\mathbf{h} \mathcal{N}(\mathbf{h}, \mathbf{0}_{2Mn}, \Sigma) \times e^{-\beta \sum_a \mathcal{L}(Q, E, R, m, d; \mathbf{h}, c, \beta_{\text{VAE}}, \lambda, \bar{\lambda})} \right)^P,
 \end{aligned}$$

where \mathbf{w}_l^* , \mathbf{w}_l^a and \mathbf{v}_l^a are column vectors of W^* , W^a , and V^a , respectively. Assuming the replica symmetric (RS) ansatz, one reads

$$Q_{ls}^{aa} = Q_{ls}, \quad E_{ls}^{aa} = E_{ls}, \quad R_{ls}^{aa} = R_{ls}, \quad m_{sl^*}^a = m_{sl^*}, \quad d_{sl^*}^a = d_{sl^*}, \quad (21)$$

$$Q_{ls}^{ab} = Q_{ls} - \frac{\chi_{ls}}{\beta}, \quad E_{ls}^{ab} = E_{ls} - \frac{\zeta_{ls}}{\beta}, \quad R_{ls}^{ab} = R_{ls} - \frac{\omega_{ls}}{\beta}, \quad (22)$$

where all parameters are denoted as $\Theta \triangleq (Q, E, R, m, d, \chi, \zeta, \omega) \in \mathbb{R}^{M \times (6M + 2M^*)}$. This RS ansatz restricts the integration of the replicated weight parameters $\{W_a, V_a\}$ across the entire $\mathbb{R}^{(2M \times N) \times n}$ to a subspace that satisfies the constraints in Eq. 21 and 22. Using the Fourier transform of the delta functions, \mathcal{S} is expanded as

$$\begin{aligned}
 \mathcal{S} &= \int d\hat{Q} d\hat{E} d\hat{R} d\hat{\chi} d\hat{\zeta} d\hat{m} d\hat{d} \prod_a dW^a dV^a e^{\frac{1}{2} \sum_{ls} \sum_a (\beta \hat{Q}_{ls} - \beta^2 \hat{\chi}_{ls}) (NQ_{ls} - \mathbf{w}_l^a \mathbf{w}_s^a) - \frac{1}{2} \sum_{ls} \sum_{a \neq b} \beta^2 \hat{\chi} (Q_{ls} - \frac{\chi_{ls}}{\beta} - \mathbf{w}_l^a \mathbf{w}_s^b)} \\
 &\quad \times e^{\frac{1}{2} \sum_{ls} \sum_a (\beta \hat{E}_{ls} - \beta^2 \hat{\zeta}_{ls}) (NE_{ls} - \mathbf{v}_l^a \mathbf{v}_s^a) - \frac{1}{2} \sum_{ls} \sum_{a \neq b} \beta^2 \hat{\zeta} (E_{ls} - \frac{\zeta_{ls}}{\beta} - \mathbf{v}_l^a \mathbf{v}_s^b)} \\
 &\quad \times e^{\sum_{ls} \sum_a (\beta \hat{R}_{ls} - \beta^2 \hat{\omega}_{ls}) (NR_{ls} - \mathbf{w}_l^a \mathbf{v}_s^a) - \sum_{ls} \sum_{a \neq b} \beta^2 \hat{\omega} (R_{ls} - \frac{\omega_{ls}}{\beta} - \mathbf{w}_l^a \mathbf{v}_s^b)} \\
 &\quad \times e^{-\sum_{ls} \sum_a \beta \hat{m}_{sl^*} (Nm_{sl^*} - \mathbf{w}_s^a \mathbf{w}_{l^*}^*) - \sum_{ls} \sum_a \beta \hat{d}_{sl^*} (Nd_{sl^*} - \mathbf{v}_s^a \mathbf{w}_{l^*}^*)} e^{-\frac{\beta \lambda}{2} \sum_a (\|W_a\|_F^2 + \|V_a\|_F^2)} \\
 &= \int d\hat{\Theta} e^{\frac{n\beta N}{2} (\text{tr}(\hat{Q}Q + (n-1)\hat{\chi}\chi - n\beta Q\hat{\chi}) + \text{tr}(\hat{E}E + (n-1)\hat{\zeta}\zeta - n\beta E\hat{\zeta}) + 2\text{tr}(\hat{R}R + (n-1)\hat{\omega}\omega - n\beta R\hat{\omega}) - \text{tr}(\hat{m}m) - \text{tr}(\hat{d}d))} \\
 &\quad \times \int dW^a dV^a e^{-\frac{\beta}{2} \sum_{ls} ((\hat{Q}_{ls} + \lambda) \sum_a \mathbf{w}_l^a \mathbf{w}_s^a + (\hat{E}_{ls} + \lambda) \sum_a \mathbf{v}_l^a \mathbf{v}_s^a + 2\hat{R}_{ls} \sum_a \mathbf{w}_l^a \mathbf{v}_s^a) + \frac{\beta^2}{2} \sum_{ls} (\hat{\chi}_{ls} (\sum_a \mathbf{w}_a)^2 + \hat{\zeta}_{ls} (\sum_a \mathbf{v}_a)^2 + 2\hat{\omega}_{ls} \sum_a \mathbf{w}_a \sum_a \mathbf{v}_a)} \\
 &\quad \times e^{\beta \sum_{ls} \hat{m}_{sl^*} \sum_a \mathbf{w}_s^a \mathbf{w}_{l^*}^* + \beta \sum_{ls} \hat{d}_{sl^*} \sum_a \mathbf{v}_s^a \mathbf{w}_{l^*}^*},
 \end{aligned}$$

where $d\hat{\Theta} \triangleq d\hat{Q} d\hat{E} d\hat{R} d\hat{\chi} d\hat{\zeta} d\hat{m} d\hat{d}$. This can be derived with the help of the identity for any symmetric positive matrix $M \in \mathbb{R}^{M \times M}$ and any vector $\mathbf{x} \in \mathbb{R}^M$, given by

$$e^{\frac{1}{2} \mathbf{x}^\top M \mathbf{x}} = \int D\xi_M e^{\xi^\top M^{\frac{1}{2}} \mathbf{x}},$$

where $D\xi_M$ is the standard Gaussian measure on \mathbb{R}^M . Then, we obtain:

$$\begin{aligned}
 \mathcal{S} &= \int d\hat{\Theta} e^{\frac{n\beta N}{2} (\text{tr}(\hat{Q}Q + (n-1)\hat{\chi}\chi - n\beta Q\hat{\chi}) + \text{tr}(\hat{E}E + (n-1)\hat{\zeta}\zeta - n\beta E\hat{\zeta}) + 2\text{tr}(\hat{R}R + (n-1)\hat{\omega}\omega - n\beta R\hat{\omega}) - \text{tr}(\hat{m}m) - \text{tr}(\hat{d}d))} \\
 &\quad \times \left(\int D\xi_{2M} \left(\int d\tilde{w} e^{\frac{\beta}{2} \tilde{w}^\top (\hat{Q} + \lambda I_{2M}) \tilde{w} + \beta (\xi_{2M}^\top \hat{\chi}^{\frac{1}{2}} + \mathbf{1}_{2M}^\top \tilde{m}) \tilde{w}} \right)^n \right)^N \\
 &= \int d\hat{\Theta} e^{\frac{n\beta N}{2} (\text{tr}(\hat{Q}Q + (n-1)\hat{\chi}\chi - n\beta Q\hat{\chi}) + \text{tr}(\hat{E}E + (n-1)\hat{\zeta}\zeta - n\beta E\hat{\zeta}) + 2\text{tr}(\hat{R}R + (n-1)\hat{\omega}\omega - n\beta R\hat{\omega}) - \text{tr}(\hat{m}m) - \text{tr}(\hat{d}d))} \\
 &\quad \times e^{N \log \int D\xi_{2M} \left(\int d\tilde{w} e^{\frac{\beta}{2} \tilde{w}^\top (\hat{Q} + \lambda I_{2M}) \tilde{w} + \beta (\xi_{2M}^\top \hat{\chi}^{\frac{1}{2}} + \mathbf{1}_{2M}^\top \tilde{m}) \tilde{w}} \right)^n} \\
 &= \int d\hat{\Theta} e^{\frac{n\beta N}{2} (\text{tr}(\hat{Q}Q - \hat{\chi}\chi) + \text{tr}(\hat{E}E - \hat{\zeta}\zeta) + 2\text{tr}(\hat{R}R - \hat{\omega}\omega) - \text{tr}(\hat{m}m) - \text{tr}(\hat{d}d) + \mathcal{O}(n))} \\
 &\quad \times e^{Nn \left(\int D\xi_{2M} \log \int d\tilde{w} e^{\frac{\beta}{2} \tilde{w}^\top (\hat{Q} + \lambda I_{2M}) \tilde{w} + \beta (\xi_{2M}^\top \hat{\chi}^{\frac{1}{2}} + \mathbf{1}_{2M}^\top \tilde{m}) \tilde{w}} + \mathcal{O}(n) \right)} \\
 &= \int d\hat{\Theta} e^{\frac{n\beta N}{2} (\text{tr}(\hat{Q}Q - \hat{\chi}\chi) + \text{tr}(\hat{E}E - \hat{\zeta}\zeta) + 2\text{tr}(\hat{R}R - \hat{\omega}\omega) - \text{tr}(\hat{m}m) - \text{tr}(\hat{d}d) + \text{tr}[(\hat{\chi}^{\frac{1}{2}})^\top (Q + \lambda)^{-1} \hat{\chi}^{\frac{1}{2}}] + \mathbf{1}_{2M}^\top \tilde{m} \tilde{Q}^{-1} \tilde{m}^\top \mathbf{1}_{2M}) + o(n) + o(N) + o(\beta)}
 \end{aligned}$$

where $\tilde{w} \triangleq (w_1, \dots, w_M, v_1, \dots, v_M)$ and

$$\tilde{Q} \triangleq \begin{pmatrix} \hat{Q} & \hat{R} \\ \hat{R} & \hat{E} \end{pmatrix}, \quad \tilde{\chi} \triangleq \begin{pmatrix} \hat{\chi} & \hat{\omega} \\ \hat{\omega} & \hat{\zeta} \end{pmatrix}, \quad \tilde{m} \triangleq \begin{pmatrix} \hat{m} & \mathbf{0}_{MM^*} \\ \mathbf{0}_{MM^*} & \hat{d} \end{pmatrix}.$$

The integral with respect to \tilde{w} can be calculated analytically using this expression. \mathcal{E} is also expanded as

$$\begin{aligned}
 \log \mathcal{E} &= \log \int \prod_a dD^a \left(\int Dc \int d\mathbf{h} \mathcal{N}(\mathbf{h}, \mathbf{0}_{2Mn}, \Sigma) e^{-\beta \sum_a \mathcal{L}(Q, E, R, m, d; \mathbf{h}, \mathbf{c}, \beta_{\text{VAE}}, \lambda, \tilde{\lambda})} \right)^P \\
 &= n \log \int dD e^{-\frac{\beta P}{2} (\text{tr}[(Q + \beta_{\text{VAE}})D] - \beta_{\text{VAE}} \text{tr}(\log D))} \\
 &\quad + P \log \int Dc \int d\mathbf{h} \mathcal{N}(\mathbf{h}, \mathbf{0}_{2Mn}, \Sigma) e^{-\beta \sum_a \mathcal{L}(Q, E, R, m, d; \mathbf{h}, \mathbf{c}, \beta_{\text{VAE}}, \lambda, \tilde{\lambda})} \\
 &= n \log \int dD e^{-\frac{\beta P}{2} (\text{tr}[(Q + \beta_{\text{VAE}})D] - \beta_{\text{VAE}} \text{tr}(\log D))} \\
 &\quad + P \log \int Dc D\xi_{2M \times 2M} \left(\int D\mathbf{z}_{2M \times 2M} e^{-\beta \mathcal{L}(Q, E, R, m, d; \xi_{2M \times 2M}, \mathbf{z}_{2M \times 2M}, \mathbf{c}, \beta_{\text{VAE}}, \lambda, \tilde{\lambda})} \right)^n \\
 &= n \log \int dD e^{-\frac{\beta P}{2} (\text{tr}[(Q + \beta_{\text{VAE}})D] - \beta_{\text{VAE}} \text{tr}(\log D))} \\
 &\quad + Pn \int Dc D\xi_{2M \times 2M} \log \int D\mathbf{z}_{2M \times 2M} e^{-\beta \mathcal{L}(Q, E, R, m, d; \xi_{2M \times 2M}, \mathbf{z}_{2M \times 2M}, \mathbf{c}, \beta_{\text{VAE}}, \lambda, \tilde{\lambda})} + o(n).
 \end{aligned}$$

Taking the limit $\beta \rightarrow \infty$, one can obtain

$$\log \mathcal{L} = -Pn\beta \int Dc D\xi_{2M \times 2M} \log \min_{D, \mathbf{z}_{2M \times 2M}} \mathcal{L}(\Theta; \mathbf{z}_{2M \times 2M}, \xi_{2M \times 2M})$$

Substituting \mathcal{S} and \mathcal{E} into the expression of the replicated partition function yields

$$\begin{aligned}
 \mathbb{E}_{\mathcal{D}} Z_{\beta}^n(\mathcal{D}) &= \int d\hat{\Theta} d\hat{\Theta} e^{\frac{n\beta N}{2} (\text{tr}(\hat{Q}Q - \hat{\chi}\chi) + \text{tr}(\hat{E}E - \hat{\zeta}\zeta) + 2\text{tr}(\hat{R}R - \hat{\omega}\omega) - \text{tr}(\hat{m}m) - \text{tr}(\hat{d}d) + \text{tr}[(\hat{\chi}^{\frac{1}{2}})^\top (Q + \lambda)^{-1} \hat{\chi}^{\frac{1}{2}}] + \mathbf{1}_{2M}^\top \tilde{m} \tilde{Q}^{-1} \tilde{m}^\top \mathbf{1}_{2M})} \\
 &\quad \times e^{-\alpha N n \beta \int Dc D\xi_{2M \times 2M} \log \min_{D, \mathbf{z}_{2M \times 2M}} \mathcal{L}(\Theta; \mathbf{z}_{2M \times 2M}, \xi_{2M \times 2M})}
 \end{aligned}$$

In the end, from the identity:

$$\lim_{n \rightarrow +0} \frac{\log \mathbb{E}_{\mathcal{D}} Z_{\beta}^n(\mathcal{D})}{n},$$

one obtains

$$f = \text{extr}_{\Theta, \hat{\Theta}} \left\{ -\frac{1}{2} \left(\text{tr}(Q\hat{Q} - \chi\hat{\chi}) + \text{tr}(E\hat{E} - \zeta\hat{\zeta}) + 2\text{tr}(R\hat{R} - \omega\hat{\omega}) - \text{tr}(m\hat{m}) - \text{tr}(d\hat{d}) \right) \right. \\ \left. - \frac{1}{2} \left(\text{tr}[(\tilde{\chi}^{\frac{1}{2}})^{\top} (\tilde{Q} + \lambda)^{-1} \tilde{\chi}^{\frac{1}{2}}] + \mathbf{1}_{2M}^{\top} \tilde{m} \tilde{Q}^{-1} \tilde{m}^{\top} \mathbf{1}_{2M} \right) + \alpha \int DcD\xi_{2M \times 2M} \log_{D, \mathbf{z}_{2M \times 2M}} \min_{D, \mathbf{z}_{2M \times 2M}} \mathcal{L}(\Theta; \mathbf{z}_{2M \times 2M}, \xi_{2M \times 2M}) \right\}. \quad (23)$$

C.2 Derivation of Claim 4.2

When $M = M^* = 1$, the following expressions holds:

$$\tilde{\chi}^{\frac{1}{2}} = \frac{1}{\sqrt{\hat{\chi} + \hat{\zeta} + 2\sqrt{\hat{\chi}\hat{\zeta} - \hat{\omega}^2}}} \begin{pmatrix} \hat{\chi} + \sqrt{\hat{\chi}\hat{\zeta} - \hat{\omega}^2} & \hat{\omega} \\ \hat{\omega} & \hat{\zeta} + \sqrt{\hat{\chi}\hat{\zeta} - \hat{\omega}^2} \end{pmatrix}, \quad \tilde{Q} = \frac{1}{\hat{Q}\hat{E} - \hat{R}^2} \begin{pmatrix} \hat{E} & -\hat{R} \\ -\hat{R} & \hat{Q} \end{pmatrix}$$

Using these, a part of the exponential function of Eq. (23) can be reduced as

$$-\frac{1}{2} \left(\text{tr}[(\tilde{\chi}^{\frac{1}{2}})^{\top} (\tilde{Q} + \lambda)^{-1} \tilde{\chi}^{\frac{1}{2}}] + \mathbf{1}_2^{\top} \tilde{m} \tilde{Q}^{-1} \tilde{m}^{\top} \mathbf{1}_2 \right) = -\frac{(\lambda + \hat{Q})(\hat{m}^2 + \hat{\chi}) + (\lambda + \hat{E})(\hat{d}^2 + \hat{\zeta}) - 2\hat{R}(\hat{m}\hat{d} + \hat{\omega})}{2((\hat{Q} + \lambda)(\hat{E} + \lambda) - \hat{R}^2)}. \quad (24)$$

We notice that \mathbf{u} and $\tilde{\mathbf{u}}$ can be expressed as

$$u_a = \sqrt{\frac{\chi - \omega}{\beta}} z_{11}^a + \sqrt{\frac{\omega}{\beta}} z_{12}^a + \sqrt{Q - R} \xi_{11} + \sqrt{R} \xi_{12}, \\ \tilde{u}_a = \sqrt{\frac{\zeta - \omega}{\beta}} z_{22}^a + \sqrt{\frac{\omega}{\beta}} z_{12}^a + \sqrt{E - R} \xi_{22} + \sqrt{R} \xi_{12},$$

where $z_{11}^a, z_{12}^a, z_{22}^a, \xi_{11}, \xi_{12}, \xi_{22}$ follows standard Gaussian distribution $\mathcal{N}(0, 1)$. By substituting \mathbf{u} and $\tilde{\mathbf{u}}$, \mathcal{E} is transformed to

$$\mathcal{E} = \int DcD\xi_{2M \times 2M} \log_{D, \mathbf{z}_{2M \times 2M}} \min_{D, \mathbf{z}_{2M \times 2M}} \mathcal{L}(\Theta; \mathbf{z}_{2M \times 2M}, \xi_{2M \times 2M}) \\ = \alpha \int DcD\xi_{11} D\xi_{12} \xi_{22} \min_{D, z_{11}, z_{12}, z_{22}} \mathcal{L}(\Theta, D; z_{11}, z_{12}, z_{22}, \xi_{11}, \xi_{12}, \xi_{22}).$$

The extremum conditions are represented as the following equations:

$$0 = \frac{\partial \mathcal{L}}{\partial z_{11}} = \sqrt{\eta(\chi - \omega)} \left(c\sqrt{\rho}d + \sqrt{\eta} \left(\sqrt{\zeta - \omega} z_{22} + \sqrt{\omega} z_{12} + \sqrt{E - R} \xi_{22} + \sqrt{R} \xi_{12} \right) \right), \\ 0 = \frac{\partial \mathcal{L}}{\partial z_{12}} = \sqrt{\eta\omega} \left((1 - (Q + \beta_{\text{VAE}})) \left(c\sqrt{\rho}d + \sqrt{\eta} \left(\sqrt{\zeta - \omega} z_{22} + \sqrt{\omega} z_{12} + \sqrt{E - R} \xi_{22} + \sqrt{R} \xi_{12} \right) \right) \right. \\ \left. + \left(c\sqrt{\rho}m + \sqrt{\eta}(\sqrt{\chi - \omega} z_{11} + \sqrt{\omega} z_{12} + \sqrt{Q - R} \xi_{11} + \sqrt{R} \xi_{12}) \right) \right) \\ 0 = \frac{\partial \mathcal{L}}{\partial z_{22}} = \sqrt{\eta(\zeta - \omega)} \left(c\sqrt{\rho}m + \sqrt{\eta} \left(\sqrt{\chi - \omega} z_{11} + \sqrt{\omega} z_{12} + \sqrt{Q - R} \xi_{11} + \sqrt{R} \xi_{12} \right) \right. \\ \left. - (Q + \beta_{\text{VAE}}) \left(z\sqrt{\rho}m z_{11} + \sqrt{\eta} \left(\sqrt{\zeta - \omega} z_{22} + \sqrt{\omega} z_{12} + \sqrt{E - R} \xi_{22} + \sqrt{R} \xi_{12} \right) \right) \right), \\ 0 = \frac{\partial \mathcal{L}}{\partial D} = (Q + \beta_{\text{VAE}}) - \frac{\beta_{\text{VAE}}}{D}.$$

Solving these equations yields the following expression:

$$\mathcal{E} = n\beta \left(\frac{(Q - \eta\chi + \beta_{\text{VAE}})(\rho d^2 + \eta E) - \eta\zeta(\rho m^2 + \eta q) + 2(\eta\omega - 1)(\rho md + \eta r)}{\eta\zeta(Q - \eta\chi + \beta_{\text{VAE}}) + (\eta\omega - 1)^2} + \beta_{\text{VAE}} \left(\log \frac{e(Q + \beta_{\text{VAE}})}{\beta_{\text{VAE}}} \right) \right) \quad (25)$$

In the end, substituting Eq. (24) and (25) into Eq. (23), one can easily obtain

$$f = \text{extr}_{\Theta} \left\{ -\frac{1}{2}(\hat{Q}Q - \chi\hat{\chi}) - \frac{1}{2}(\hat{E}E - \zeta\hat{\zeta}) - (\hat{R}R - \omega\hat{\omega}) + \hat{m}m + \hat{d}d \right. \\ \left. + \frac{(\lambda + \hat{E})(\hat{m}^2 + \hat{\chi}) + (\lambda + \hat{Q})(\hat{d}^2 + \hat{\zeta}) - 2\hat{R}(\hat{m}\hat{m} + \hat{\omega})}{2\hat{G}} - \frac{\alpha}{2} \left(\frac{(Q - \eta\chi + \beta_{\text{VAE}})(\rho d^2 + \eta E) - \eta\zeta(\rho m^2 + \eta Q)}{G} \right. \right. \\ \left. \left. + \frac{2(\eta\omega - 1)(\rho md + \eta r)}{G} + \beta_{\text{VAE}} \log \frac{e(Q + \beta_{\text{VAE}})}{\beta_{\text{VAE}}} \right) \right\},$$

C.3 Derivation of Claim 5.1

From the expansion in the first order term with respect to α , one obtains the following solution:

$$Q = E = R = \chi = \zeta = \omega = m = d = 0 \quad (\rho + \eta \leq \beta_{\text{VAE}}), \quad (26)$$

$$Q = \eta + \rho - \beta_{\text{VAE}}, \quad E = \frac{\eta + \rho - \beta_{\text{VAE}}}{(\eta + \rho)^2}, \quad \chi = \zeta = \omega = 0, \quad m = \sqrt{\eta + \rho - \beta_{\text{VAE}}}, \quad d = \frac{\eta + \rho - \beta_{\text{VAE}}}{\eta + \rho} \quad (\rho + \eta > \beta_{\text{VAE}}). \quad (27)$$

Note that one can evaluate $\lim_{\beta \rightarrow \infty} \mathbb{E}_{\mathcal{D}} \mathbb{E}_p(W, V, D; \mathcal{D}, \beta) \epsilon_g(W, W^*)$ as $\rho - 2\sqrt{\rho m} + Q$. Thus, one obtains

$$\epsilon_g = \begin{cases} \rho - \sqrt{\eta + \rho - \beta_{\text{VAE}}}(2\sqrt{\rho} - \sqrt{\eta + \rho - \beta_{\text{VAE}}}) & (\rho + \eta \leq \beta_{\text{VAE}}) \\ 1 & (\rho + \eta > \beta_{\text{VAE}}) \end{cases}. \quad (28)$$

The optimal condition for β_{VAE} yields optimal value $\beta_{\text{VAE}}^* = \eta$.

C.4 Derivation of Claim 5.2

We first notice that rate and distortion can be expressed as

$$R_* = \mathbb{E}_{\mathcal{D}} R(\bar{W}(\mathcal{D}), \bar{V}(\mathcal{D}), \bar{D}(\mathcal{D})) = \frac{1}{2} \left(\rho d^2 + \eta E + \frac{\beta_{\text{VAE}}}{Q + \beta_{\text{VAE}}} - 1 - \log \frac{\beta_{\text{VAE}}}{Q + \beta_{\text{VAE}}} \right), \quad (29)$$

$$D_* = \mathbb{E}_{\mathcal{D}} D(\bar{W}(\mathcal{D}), \bar{V}(\mathcal{D}), \bar{D}(\mathcal{D})) = \frac{1}{2} \left(\rho + \eta - 2(\rho md + \eta R) + Q \left((\rho d^2 + \eta E) + \frac{\beta_{\text{VAE}}}{Q + \beta_{\text{VAE}}} \right) \right), \quad (30)$$

respectively. Then, substituting Eq. (26) and (26) into Eq. (29) and Eq. (30), one can obtain

$$R_* = \begin{cases} \frac{1}{2} \log \frac{\eta + \rho}{\beta_{\text{VAE}}} & \rho + \eta \leq \beta_{\text{VAE}} \\ 0 & \rho + \eta > \beta_{\text{VAE}} \end{cases}, \\ D_* = \begin{cases} \frac{\beta_{\text{VAE}}}{2} & \rho + \eta \leq \beta_{\text{VAE}} \\ \frac{\rho + \eta}{2} & \rho + \eta > \beta_{\text{VAE}} \end{cases}.$$

From these equations, one obtains

$$R(D^*) = \begin{cases} \frac{1}{2} \log \frac{\rho + \eta}{2D^*} & 0 \leq D^* < \frac{\eta + \rho}{2} \\ 0 & D^* \geq \frac{\rho + \eta}{2} \end{cases}.$$